

48. Synthesis and X-Ray Analysis of a Nickel Triphenyl-Cyclopropenyl Complex. A MO-Interpretation of the Geometry and Bonding in the $(C_3H_3)ML_3$ -Type of Complexes

by Carlo Mealli¹⁾ and Stefano Midollini

Istituto per lo Studio della Stereochimica ed Energetica dei Composti di Coordinazione, C.N.R.,
Via Guerrazzi 27, 50132 Florence, Italy

and Simonetta Moneti

Istituto di Chimica Generale dell'Università, Via Nardi 39, 50132 Florence, Italy

and Thomas A. Albright

Department of Chemistry, University of Houston, Texas 77004, U.S.A.

(11.VIII.82)

Summary

The reaction of $[(C_3Ph_3)Ni(PPh_3)_2]ClO_4$ with $P(CH_2CH_2PPh_2)_3(pp_3)$ and $NaBPh_4$ yields the $[(C_3Ph_3)Ni(pp_3)]BPh_4$ -complex. After long exposure of the solution of this compound in acetone/butanol to the air a new derivative $[(C_3Ph_3)Ni(pp_2po)]BPh_4 \cdot 0.5 C_4H_9OH$, where pp_2po is $(Ph_2PCH_2CH_2)_2P(CH_2CH_2POPh_2)$, is obtained. Complete X-ray analysis has been carried out for the latter complex: $a = 18.303$ (5); $b = 29.445$ (6); $c = 13.305$ (5) Å, $\beta = 112.70$ (9)°; space group monoclinic, $P2_1/a$, $Z = 4$. Disorder problems were encountered in the refinement of the structure. The best R is 0.093. One of the arms of the parent pp_3 -molecule, not coordinated to the metal, undergoes oxidation. The Ni-atom, coordinated by the three remaining P-atoms of the ligand, is also linked in a roughly η^3 -mode to the cyclopropenium ligand. The geometry of the molecule is examined in detail. Extended HMO-calculations were performed to interpret how the variation of P-Ni-P angles affects the bonding between the NiP_3 - and C_3H_3 -fragments. The conclusion is that the overall energy of the complex may be lowered in spite of a weakening of the Ni-cyclopropenium linkage. Extensions are made to other systems containing a linkage between a metal and a X_3 -ring ($X = P, As$).

1. Introduction. – In the presence of ML_2 -fragments such as $M(PPh_3)_2$ ($M = Ni, Pd, Pt$) fluxional behavior for the synthesized $[(C_3Ph_3)M(PPh_3)_2]^+$ -cations has been ascertained [1]. The structural determination of four of these 16-valence-electron derivatives has enabled us to determine the structural profile for the ring-whizzing motion of the ML_2 -group over the cyclopropenium ring. We have also shown [2]

¹⁾ Author to whom correspondence should be addressed.

that tridentate ligands having N, P, or As donor atoms easily substitute the two triphenylphosphine groups in the above type of compounds to give stable η^3 -coordinated complexes of type $[(C_3Ph_3)ML]^+$, which have the closed-shell 18-electron configuration.

We report now on the reactivity of the potential tetradentate, tripod-like ligand tris(2-diphenylphosphinoethyl)phosphine (pp_3) toward the $[(C_3Ph_3)Ni(PPh_3)_2]^+$ -cation. The structural and spectroscopic characterization of $[(C_3Ph_3)Ni(pp_2po)]\cdot BPh_4 \cdot 0.5 C_4H_9OH$, where pp_2po is the new ligand, synthesized *in situ* [bis(2-diphenylphosphinoethyl)](2-diphenylphosphinoxidoethyl)phosphine, is reported along with a discussion of the bonding in this type of complexes.

2. Experimental. – 2.1. *Synthesis.* The reagent-grade solvents were dried by usual procedures. The ligand pp_3 (= tris(2-diphenylphosphinoethyl)phosphine) was purchased from the *Pressure Chemical Co.*, Pittsburgh, Pa, and used without further purification. The complex $[(C_3Ph_3)Ni(PPh_3)_2]ClO_4$ was prepared as previously described [1].

^{31}P -NMR. spectra were taken in CD_2Cl_2 -solutions and recorded at 32.2 MHz on a *CFT 20 Varian* spectrometer with proton noise decoupling. The other physical measurements were executed by the procedures described in [3].

Preparation of $[(C_3Ph_3)Ni(pp_3)]BPh_4 \cdot 0.5 CH_2Cl_2$. The reaction was performed under N_2 . The ligand pp_3 (1 mmol) in 15 ml of CH_2Cl_2 was added at r.t. to a solution of $[(C_3Ph_3)Ni(PPh_3)_2]ClO_4$ (1 mmol) in CH_2Cl_2 (15 ml). Sodium tetraphenylborate (1 mmol) in EtOH (20 ml) was added and a fast stream of N_2 was passed through the solution until crystallization began. The thin, yellow crystals were filtered, washed with EtOH and light petroleum, and dried in a stream of dry N_2 .

$C_{87}H_{77}BNiP_4 \cdot 0.5 CH_2Cl_2$ Calc. C 77.36 H 5.78 Ni 4.32% Found C 76.88 H 5.84 Ni 4.30%

Preparation of $[(C_3Ph_3)Ni(pp_2po)]BPh_4 \cdot 0.5 C_4H_9OH$ ($pp_2po = (Ph_2POCH_2CH_2)P(CH_2CH_2PPh_2)_2$). The above compound (0.5 mmol) was dissolved in acetone (20 ml) at 50°. After addition of butanol (20 ml) and exposition of the resulting solution to the air for about one week at r.t., some large orange-brown crystals together with thin, yellow ones precipitated. The large crystals were separated by decantation, washed with butanol and petroleum ether and dried *in vacuo*. By repeated crystallizations only the crystals of the pp_2po -derivative were obtained.

$C_{87}H_{77}BNiOP_4 \cdot 0.5 C_4H_{10}O$ Calc. C 78.12 H 6.04 Ni 4.29% Found C 77.59 H 6.91 Ni 4.37%

2.2. *Crystal data and data collection.* Crystals of $[(C_3Ph_3)Ni(pp_2po)]BPh_4 \cdot 0.5 C_4H_9OH$ are monoclinic, space group $P2_1/a$, $a = 18.303$ (5), $b = 29.445$ (6), $c = 15.305$ (5) Å, $\beta = 112.70$ (9)°, $D_x = 1.19$ gcm $^{-3}$. Diffraction measurements were made with a crystal of dimensions $0.20 \times 0.21 \times 0.18$ mm 3 on a *Philips PW 1100* automated diffractometer [4] using graphite monochromatized *MoK α* radiation. A total of 7619 reflections (2912 with $I \geq 3\sigma(I)$) were measured up to $\theta = 20^\circ$. No crystal decay was detected from behavior of three standard reflections. The data were corrected for absorption. The transmission coefficients varied between 0.92 and 0.86 ($\mu = 3.82$ for *MoK α*).

2.3. *Structure analysis and refinement.* The structure was solved and refined with the *SHELX-76* system of programs. Direct methods and a series of F_0 - and ΔF -maps enabled us to determine the positions of all non-H-atoms. However, the ligand arm containing the phosphine-oxide group that is not bonded to the metal and the butanol molecule give broad, weak peaks. During the least-squares refinement the temperature factors of the atoms P(4), O(1), C(95), C(96), C(25)–C(30), and C(31)–C(36), rose to abnormally high values. Attempts were made to refine the ill-behaving atoms in split positions, but with little improvement of convergence. However, the most significant chemical information is not heavily affected by the disorder. No unreasonable bond distances or angles were calculated from the refined atomic parameters. Only the Ni-, P(1)-, P(2)- and P(3)-atoms were assigned anisotropic temperature factors. All the phenyl groups were refined as rigid bodies, with H-atoms introduced in the final least-squares cycles at calculated positions (C–H, 0.95 Å). The butanol molecule was refined with a population parameter of 0.5 in accordance with results of elemental analysis. In this manner the temperature factors are also kept reasonably low. Final $R = 0.093$ ($R_w = 0.101$). Atomic parameters are reported in *Table 1*.

Table 1. Atomic parameters for $[(C_3Ph_3)Ni(pp_2po)]BPh_4 \cdot 0.5 C_4H_9OH$ (coordinates multiplied by 10^4 , temperature factors by 10^3 ; the atoms marked with * belong to solvent and were assigned population parameters of 0.5)

Atom	x	y	z	U (Å ²)	Atom	x	y	z	U (Å ²)
N(1)	2145 (1)	1107 (1)	2247 (2)	50 (2)	C(35)	4454 (14)	3033 (9)	5469 (15)	217 (14)
P(1)	3196 (3)	1117 (2)	1794 (4)	50 (4)	C(36)	4270 (14)	2587 (9)	5613 (15)	179 (14)
P(2)	1665 (3)	395 (2)	2392 (4)	44 (4)	C(37)	1839 (8)	2215 (5)	2162 (8)	60 (6)
P(3)	3062 (3)	1003 (2)	3719 (4)	64 (4)	C(38)	1922 (8)	2464 (5)	1430 (8)	79 (7)
P(4)	3415 (5)	1934 (3)	6109 (6)	136 (3)	C(39)	2093 (8)	2927 (5)	1546 (8)	94 (8)
O(1)	2531 (10)	1872 (6)	5999 (12)	164 (6)	C(40)	2180 (8)	3141 (5)	2393 (8)	79 (7)
B(1)	1527 (13)	4621 (8)	3335 (16)	51 (7)	C(41)	2097 (8)	2892 (5)	3125 (8)	90 (8)
C(91)	4068 (11)	970 (6)	3687 (13)	52 (6)	C(42)	1927 (8)	2429 (5)	3009 (8)	63 (6)
C(92)	3983 (11)	769 (6)	2706 (14)	52 (6)	C(43)	773 (8)	1436 (4)	256 (12)	74 (7)
C(93)	2935 (12)	412 (7)	4099 (14)	65 (6)	C(44)	798 (8)	1078 (4)	-328 (12)	93 (8)
C(94)	2031 (11)	309 (6)	3696 (13)	50 (6)	C(45)	362 (8)	1102 (4)	-1302 (12)	116 (9)
C(95)	3043 (17)	1389 (9)	4520 (15)	130 (11)	C(46)	-98 (8)	1484 (4)	-1692 (12)	112 (9)
C(96)	3687 (16)	1444 (8)	5525 (18)	154 (13)	C(47)	-122 (8)	1843 (4)	-1108 (12)	124 (10)
C(81)	1643 (11)	1739 (7)	2005 (14)	56 (6)	C(48)	313 (8)	1819 (4)	-134 (12)	97 (8)
C(82)	1257 (11)	1425 (7)	1307 (15)	59 (6)	C(49)	539 (10)	1374 (5)	2546 (8)	61 (6)
C(83)	1152 (11)	1420 (7)	2158 (14)	54 (6)	C(50)	-256 (10)	1321 (5)	1955 (8)	79 (7)
C(1)	3154 (7)	896 (4)	672 (11)	43 (5)	C(51)	-833 (10)	1302 (5)	2340 (8)	105 (9)
C(2)	2634 (7)	1109 (4)	-145 (11)	65 (6)	C(52)	-614 (10)	1337 (5)	3318 (8)	105 (9)
C(3)	2544 (7)	943 (4)	-1035 (11)	89 (8)	C(53)	182 (10)	1389 (5)	3910 (8)	121 (10)
C(4)	2973 (7)	564 (4)	-1108 (11)	73 (7)	C(54)	758 (10)	1408 (5)	3524 (8)	92 (8)
C(5)	3493 (7)	350 (4)	-291 (11)	65 (6)	C(55)	1468 (6)	4442 (4)	2258 (9)	57 (6)
C(6)	3583 (7)	516 (4)	599 (11)	61 (6)	C(56)	2148 (6)	4380 (4)	2068 (9)	63 (6)
C(7)	3741 (7)	1646 (5)	1894 (9)	42 (5)	C(57)	2086 (6)	4212 (4)	1188 (9)	62 (6)
C(8)	3669 (7)	1985 (5)	2491 (9)	62 (6)	C(58)	1344 (6)	4110 (4)	499 (9)	73 (7)
C(9)	4142 (7)	2373 (5)	2663 (9)	80 (7)	C(59)	664 (6)	4172 (4)	689 (9)	72 (7)
C(10)	4688 (7)	2421 (5)	2236 (9)	79 (7)	C(60)	726 (6)	4338 (4)	1568 (9)	75 (7)
C(11)	4760 (7)	2082 (5)	1638 (9)	80 (7)	C(61)	785 (8)	4998 (5)	3168 (8)	45 (5)
C(12)	4287 (7)	1694 (5)	1467 (9)	77 (7)	C(62)	556 (8)	5293 (5)	2395 (8)	67 (7)
C(13)	1962 (7)	-121 (5)	1956 (9)	51 (6)	C(63)	-31 (8)	5617 (5)	2277 (8)	90 (8)
C(14)	1749 (7)	-550 (5)	2169 (9)	83 (7)	C(64)	-389 (8)	5645 (5)	2931 (8)	69 (7)
C(15)	1985 (7)	-939 (5)	1827 (9)	101 (9)	C(65)	-161 (8)	5350 (5)	3703 (8)	62 (6)
C(16)	2434 (7)	-899 (5)	1273 (9)	76 (7)	C(66)	426 (8)	5027 (5)	3822 (8)	55 (6)
C(17)	2646 (7)	-471 (5)	1059 (9)	76 (7)	C(67)	1429 (7)	4197 (4)	3985 (10)	60 (6)
C(18)	2410 (7)	-82 (5)	1401 (9)	52 (6)	C(68)	1680 (7)	4254 (4)	4962 (10)	75 (7)
C(19)	608 (7)	296 (4)	2028 (7)	42 (5)	C(69)	1540 (7)	3913 (4)	5512 (10)	74 (7)
C(20)	267 (7)	185 (4)	2673 (7)	55 (6)	C(70)	1148 (7)	3516 (4)	5084 (10)	75 (7)
C(21)	-545 (7)	102 (4)	2352 (7)	71 (7)	C(71)	897 (7)	3460 (4)	4107 (10)	84 (7)
C(22)	-1016 (7)	130 (4)	1388 (7)	76 (7)	C(72)	1038 (7)	3800 (4)	3557 (10)	68 (7)
C(23)	-674 (7)	242 (4)	744 (7)	65 (7)	C(73)	2390 (7)	4888 (5)	3835 (9)	59 (6)
C(24)	138 (7)	324 (4)	1064 (7)	47 (6)	C(74)	2465 (7)	5355 (5)	3730 (9)	65 (6)
C(25)	4076 (14)	1839 (7)	7294 (11)	117 (9)	C(75)	3210 (7)	5559 (5)	4107 (9)	84 (8)
C(26)	4871 (14)	1963 (7)	7591 (11)	154 (12)	C(76)	3880 (7)	5297 (5)	4590 (9)	88 (8)
C(27)	5363 (14)	1941 (7)	8549 (11)	170 (13)	C(77)	3806 (7)	4831 (5)	4695 (9)	84 (7)
C(28)	5061 (14)	1794 (7)	9209 (11)	164 (12)	C(78)	3061 (7)	4626 (5)	4317 (9)	79 (7)
C(29)	4266 (14)	1670 (7)	8912 (11)	175 (13)	O(2*)	1367 (37)	2260 (20)	6379 (51)	72 (27)
C(30)	3774 (14)	1693 (7)	7955 (11)	147 (12)	C(84*)	2951 (28)	2704 (16)	9535 (34)	150 (17)
C(31)	3590 (14)	2495 (9)	5786 (15)	126 (11)	C(85*)	1526 (29)	2196 (16)	7308 (39)	142 (18)
C(32)	3095 (14)	2849 (9)	5817 (15)	130 (11)	C(86*)	2076 (28)	2514 (16)	7831 (37)	146 (17)
C(33)	3280 (14)	3295 (9)	5674 (15)	136 (12)	C(87*)	2352 (29)	2399 (16)	8868 (37)	155 (18)
C(34)	3959 (14)	3387 (9)	5500 (15)	229 (17)					

2.4. *Extended HMO-calculations.* All the calculations were carried out by using the program *ICON* [5] implemented on a *SEL 32/70* computer. The atomic parameters are those used in [1a]. The calculations on $[(C_3H_3)Ni(PH_3)_3]^+$ employed C–C, C–H, Ni–P, Ni–C and P–H bond lengths of 1.42, 1.09, 2.25, 1.970 and 1.40 Å, respectively. The H–P–H angles were set at ideal tetrahedral values.

3. Synthesis and characterization. – The $[(C_3Ph_3)Ni(PPh_3)_2]ClO_4$ -cyclopropenyl derivative reacts at r.t. with the tetradentate tripod-like ligand pp_3 in CH_2Cl_2 -solution to form the complex $[(C_3Ph_3)Ni(pp_3)]BPh_4 \cdot 0.5 CH_2Cl_2$.

The compound $[(C_3Ph_3)Ni(pp_3)]BPh_4$ is a diamagnetic yellow microcrystalline substance; it is air-stable and soluble in organic solvents such as CH_2Cl_2 , THF, acetone in which it behaves as a 1:1-electrolyte. The room-temperature ^{31}P -NMR spectrum of the complex in acetone solution shows a multiplet at $\delta = 49$ and two doublets at $\delta = 36.5$, $J_{PP} = 32$ Hz, and at $\delta = -12.2$, $J_{PP} = 23$ Hz, respectively (chemical shifts are reported as being positive for resonance downfield of 85% external H_3PO_4). The multiplet can be attributed to the coordinated apical P-atom, while the doublets are due to the two coordinated and to the uncoordinated terminal pp_3 -P-atoms, respectively. The spectrum at -80° is practically unchanged. A similar pattern has been found in the low-temperature ^{31}P -NMR spectrum of the $(NO)Rh(pp_3)$ -compound [6] (neglecting the coupling with the Rh-atom) in which the pp_3 -ligand also acts as tridentate.

Repeated crystallizations in air, at 50° , from acetone/butanol, performed to prepare suitable crystals for X-ray analysis, yielded large orange-brown crystals of formula $[(C_3Ph_3)Ni(pp_2po)]BPh_4 \cdot 0.5 C_4H_9OH$. The IR spectrum of this complex shows a strong band at 1170 cm^{-1} attributable to the P=O-stretching vibration.

4. Description of the structure. – Selected bond distances and angles for the complex $[(C_3Ph_3)Ni(pp_2po)]BPh_4 \cdot 0.5 C_4H_9OH$ are reported in Table 2. Figure 1

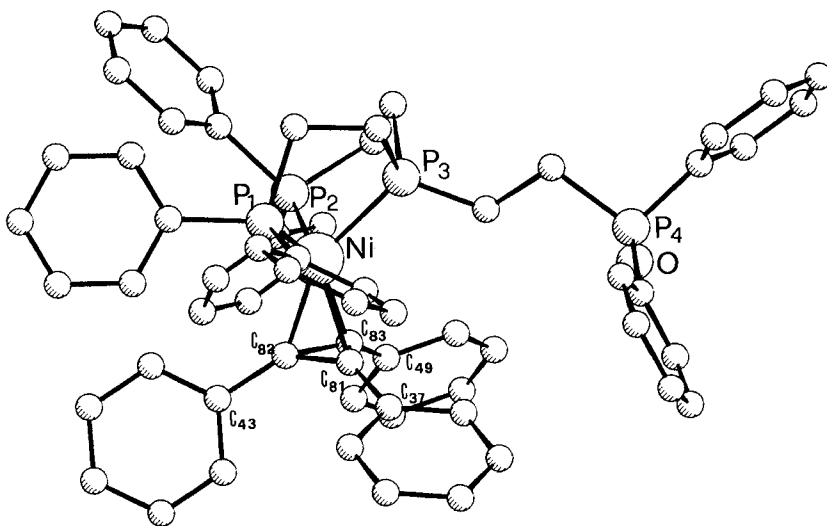


Fig. 1. A view of the $[(C_3Ph_3)Ni(pp_2po)]^+$ -complex

Table 2. Selected bond distances (\AA) and angles (deg)

Ni–P(1)	2.282 (6)	P(1)–Ni–P(2)	115.9 (2)
Ni–P(2)	2.317 (6)	P(1)–Ni–P(3)	85.2 (2)
Ni–P(3)	2.251 (6)	P(2)–Ni–P(3)	86.9 (2)
Ni–C(81)	2.048 (19)	P(1)–Ni–C(81)	107.8 (6)
Ni–C(82)	1.946 (19)	P(1)–Ni–C(82)	109.3 (6)
Ni–C(83)	1.997 (19)	P(1)–Ni–C(83)	145.6 (6)
C(81)–C(82)	1.383 (23)	P(2)–Ni–C(81)	132.8 (6)
C(81)–C(83)	1.380 (24)	P(2)–Ni–C(82)	105.5 (6)
C(82)–C(83)	1.387 (24)	P(2)–Ni–C(83)	93.2 (6)
C(81)–C(37)	1.442 (25)	P(3)–Ni–C(81)	114.4 (6)
C(82)–C(43)	1.507 (26)	P(3)–Ni–C(82)	153.1 (6)
C(83)–C(49)	1.464 (25)	P(3)–Ni–C(83)	115.9 (6)
		C(81)–Ni–C(82)	40.4 (7)
		C(81)–Ni–C(83)	39.9 (7)
		C(82)–Ni–C(83)	41.2 (7)
Tilt angles of phenyl groups (deg)			
C(81)–C(37)	25.0		
C(82)–C(43)	30.7		
C(83)–C(49)	25.1		

shows a drawing of the complex cation. One of the arms of the originally tetradentate pp_3 -ligand, not coordinated to the metal, has undergone oxidation, and it is involved in strong H-bonding ($\text{O} \dots \text{O}$, 2.67 \AA) with the butanol molecule. The structure appears to show a great deal of disorder in this region. We attribute this to the fact that the solvent is not stoichiometric and the transformation to phosphine oxide, favored by the H-bonding network, is not completed.

The Ni-atom is therefore coordinated by the central P(3)-atom and by two terminal atoms, P(1) and P(2), of the tripodal ligand. The NiP_3 -fragment is bound in a η^3 -fashion to cyclopropenium in a staggered conformation. The three P–Ni–P angles are not equal, the two involving the P(3)-atom being close to 90° (85.2 (2) $^\circ$ and 86.9 (2) $^\circ$), respectively, while the third angle (P(1)–Ni–P(2)) opens up to 115.9 (2) $^\circ$. With such a geometry the NiP_3 -moiety rather than being hemioctahedral, closely resembles the one derived from a trigonal bipyramid after removal of one axial and one equatorial donor. This is not imposed by the steric requirements of the polydentate ligand as the parent tridentate ligand $\text{PPh}_2\text{CH}_2\text{CH}_2\text{PPhCH}_2\text{PPh}_2$ (ppp) is found to form an almost regular hemioctahedron with three P–Ni–P angles close to 90° in the dimeric $[\text{Fe}_2(\mu\text{-SH})_3(\text{ppp})_2]^+$ -complex [7]. Figure 2a–c show top and side views of the inner coordination sphere about the Ni-atom. The three Ni,C-bonds are slightly different, the shortest (1.946 (19) \AA), Ni,C_a-bond, being *trans* to the Ni,P-bond formed by the central P(3)-atom of the polydentate ligand. The difference between the other two Ni–C distances (1.997 (19) and 2.048 (19) \AA) is in our opinion significant. It is accompanied by a rocking displacement of the NiP_3 -moiety with respect to the cyclopropenium ligand: P(2) lies closer to the C₃-ring (cyclopropenium) than P(1). This displacement can be viewed as a rotation about the Ni,P(3)-bond (approximately 8°) which lowers P(2) and raises P(1). The shorter Ni,C_c-bond is *cis* to the Ni,P(2)-bond. The P(3)-atom is farthest from

the C_3 -plane; the Ni,P-bond forms an angle of 128.9° with the line joining the Ni-atom and the center of the C_3 -ring, while in a C_{3v} -complex with P–Ni–P angles of 90° this angle should only be *ca.* 125° . As previously observed [1], the tilt angles of the exocyclic C, C-bonds decrease as the metal-to-ring-C-atom increases.

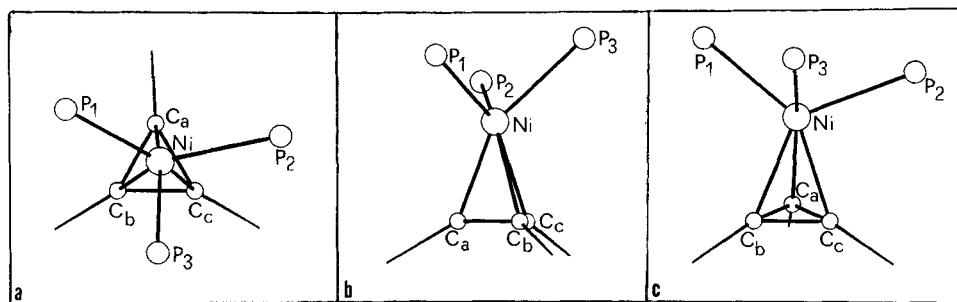


Fig. 2. a) Top view of the inner skeleton C_3NiP_3 : atoms C_a , C_b and C_c correspond in the order to the atoms labeled $C(82)$, $C(81)$ and $C(83)$ in the parameters of Table 1; b) the same moiety as viewed normal to the plane defined by the P_3 , Ni and C_a atoms; c) with respect to view b: 90° rotation about the line joining the Ni-atom and the center of the C_3 -ring.

5. Analysis of the bonding in $L_3M(C_3H_3)$ -complexes. – The analysis of the bonding in $L_3M(C_3Ph_3)$ -complexes [8] in terms of fragment-orbital interactions [9] has been extensively used to investigate some geometrical trends in these complexes. Figure 3a shows the familiar [10] six orbitals of the $Ni(PH_3)_3$ -fragment having C_{3v} -symmetry and P–Ni–P angles equal to 90° . At the bottom there are three orbitals descending from the t_{2g} -set of the octahedron; above two e_g -orbitals which are tilted and hybridized toward the missing ligands; finally at high energy there is a metal sp-hybrid. Figure 3c shows the frontier orbitals (D_{3h}) of the $C_3H_3^+$ -cation. There is a low-lying orbital of a_2'' -symmetry, and e' , σ -set and an empty π^* , e'' -set. The MO's for the molecule are shown in Figure 3b. The $2e$ -level, **1**, is the HOMO: it has a predominantly metal-d-character because there is a relatively large energy gap between the interacting e-sets. Nonetheless the overlap ensures enough bonding between the two fragments. The interactions delocalizes charge from the metal to cyclopropenium. The bonding is slightly reinforced by a three-orbital interaction of a_1 -symmetry, namely the cyclopropenium a_2'' -orbital, the metal- d_{z^2} ($1a_1$) and the sp-hybrid ($2a_1$). In spite of the four-electron destabilizing interaction between the two former orbitals, the presence of the metal empty hybrid ensures some back-donation to the metal, although limited. The interaction diagram in Figure 3 is apt to describe the bonding in the $[(\text{triphos})Ni(C_3Ph_3)]^+-$, (triphos = $CH_3C(CH_2PPh_2)_3$) complex previously reported [2]. The tripod ligand triphos constrains the P–Ni–P angles to be 90° . The complex may be considered isoelectronic with $(CO)_3Co(C_3Ph_3)$ -compound [11]. Here the OC–Co–CO angles average 104.5 (8) $^\circ$. The effect of opening the angle at the metal in ML_3 -fragments is known [10a] [12] [13]: a continuous lowering in energy of the metal- $2e$ -set, due to the loss of σ -antibonding between the ligand lone pairs and the metal- d_{xz} , d_{yz} -orbitals. For acceptor ligands such as phosphine or carbonyl molecules there is also

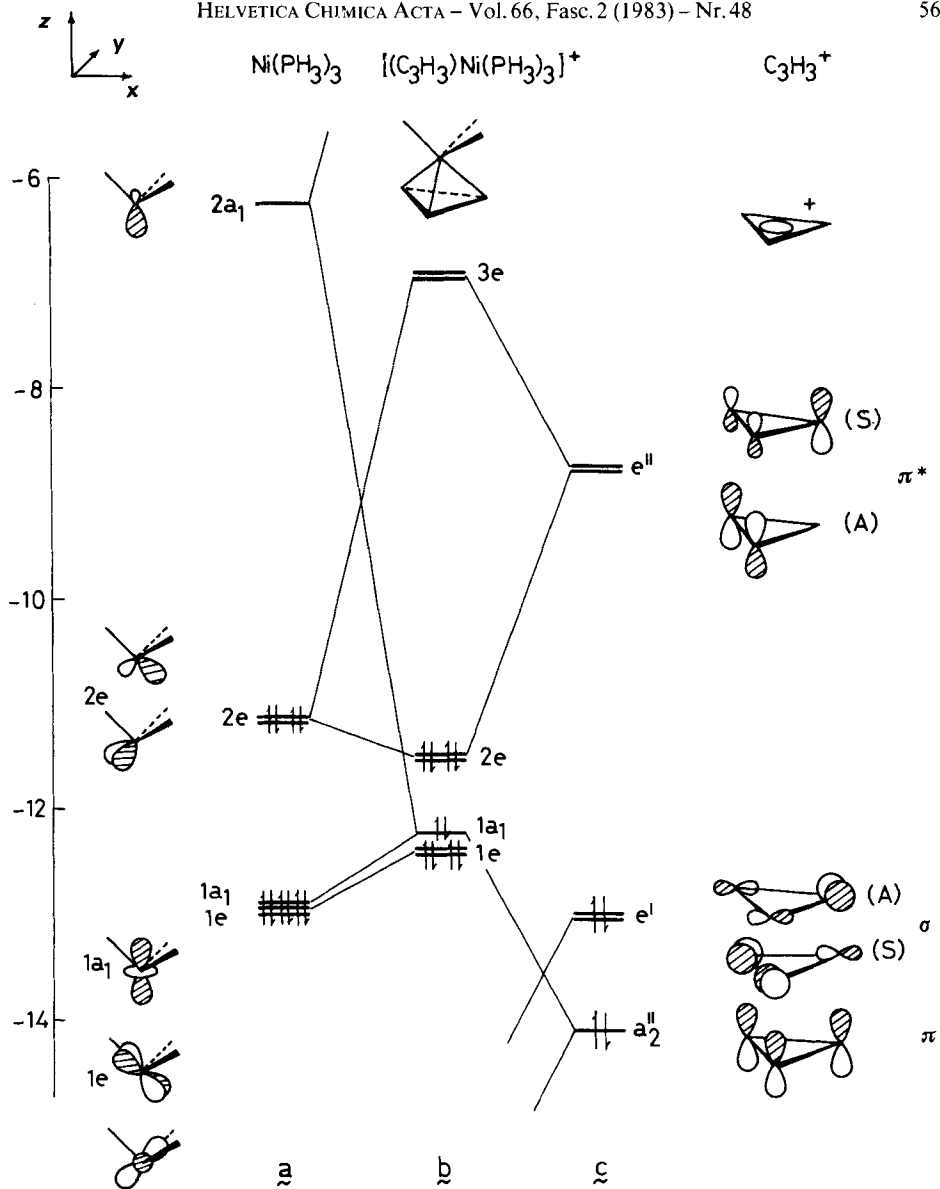
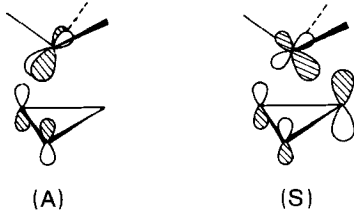


Fig. 3. Interaction diagram for $[(\text{C}_3\text{H}_3)\text{Ni}(\text{PH}_3)_3]^+$ with C_{3v} -symmetry and $P\text{-Ni-P}$ angles of 90° . a) Valence orbitals of the $\text{Ni}(\text{PH}_3)_3$ -fragment; b) MO-levels for the complex; c) Valence orbitals of the C_3H_3^+ -cation; the labels are appropriate for D_{3h} -symmetry



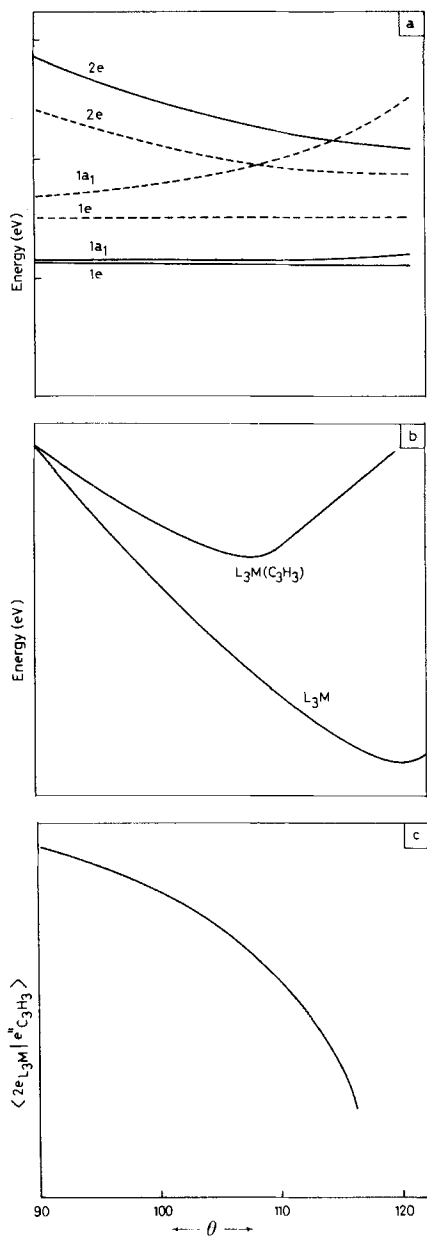
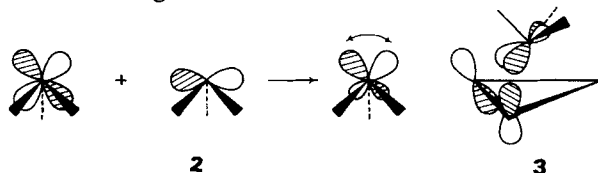


Fig. 4. a) Orbital energy variation in the $Ni(PH_3)_3$ -fragment (solid lines) and in the $[(C_3H_3)Ni(PH_3)_3]^+$ -complex (dashed lines) as a function of the θ -value of the three $P-Ni-P$ angles; C_{3v} -symmetry is maintained; b) total energy variation of the $Ni(PH_3)_3$ -fragment and of the $[(C_3H_3)Ni(PH_3)_3]^+$ -complex as a function of the θ -angle (The E -value for $Ni(PH_3)_3$ at $\theta = 90^\circ$ has been arbitrarily made coincident with that for the complex); c) variation of the overlap between the two fragment orbitals $2e_{Ni(PH_3)_3}$ and $e'_{C_3H_3}$ as a function of θ (The abscissa values are in arbitrary scale)

increasing stability on account of increasing π -back-bonding to the ligands. *Figure 4a* shows the energy variation of both the $\text{Ni}(\text{PH}_3)_3$ -levels and the levels of the $[(\text{C}_3\text{H}_3)\text{Ni}(\text{PH}_3)_3]^+$ -complex on the opening of the P–Ni–P angle from 90° to 120° . In both cases the two 2e-levels have curves which are almost parallel to $\theta = 110^\circ$. *Figure 4b* shows the total energy variation of the complex and that of the metal fragment on a relative scale. For the fragment a trigonal ($\theta = 120^\circ$) optimum is found. A minimum lies at $\theta = 108^\circ$ for the complex. Thus, the dominant driving force which opens up the P–Ni–P angles in the molecule from 90° is the stabilization of 2e. However, as this distortion occurs, the bonding of the cyclopropenium to the ML_3 -fragment diminishes. Therefore, an optimum-angle intermediate between the octahedral (90°) and trigonal (120°) extremes is found. The reason why the cyclopropenium- ML_3 interaction is weakened as θ increases from 90° is easily described in terms of perturbation theory arguments [14]: the increase of the gap between the combining e-levels, **1**, which is accompanied by a large decrease of their overlap (see *Figure 4c*). The overlap decreases because when the ML_3 -fragment becomes more planar, it acquires more $(xy, x^2 - y^2)$ -character in place of the initially predominant (xz, yz) -character. The percentage of (p_x, p_y) -hybridization in the metal 2e-set also decreases significantly [10a] [12] [13]. This latter fact does not weaken the overlap of 2e to the cyclopropenium e'' -set. As shown in **2** the hybridization opens the angle between the metal d-orbital lobes, which now span a region larger than that spanned by the cyclopropenium π^* . It has been shown [12] that a possibility for the system to increase overlap is to bend back the exocyclic C, C-bonds at the C_3 -ring to reorient the C-p-orbitals as shown in **3**. For symmetrically η^3 -bonded complexes the largest tilt (25.7° , average) is found in the $[(\text{triphos})\text{Ni}(\text{C}_3\text{Ph}_3)]^+$ -complex [2] where the θ -angle of 90° creates the largest metal-d-hybridization. The CpNi -fragment which differs from other ML_3 -fragments in having the upper 2e-level less hybridized [12] also forms an η^3 -adduct to cyclopropenium [15]. In this case the tilt of the exocyclic C, C-bonds (19.7°) is diminished and the Ni, C-bonds are among the shortest found.



Although a ligand such as pp_3 (or pp_2po) may sterically allow the formation of three P–Ni–P angles of 90° , one of the angles opens up to 116° . *Figure 5a* shows the energy variation of the MO-levels both in the $\text{Ni}(\text{PH}_3)_3$ -fragment and in the complex with cyclopropenium as function of the angle φ , defined in **4**. The 2e-set, degenerate at $\varphi = 90^\circ$, splits into symmetric (S) and antisymmetric (A) components



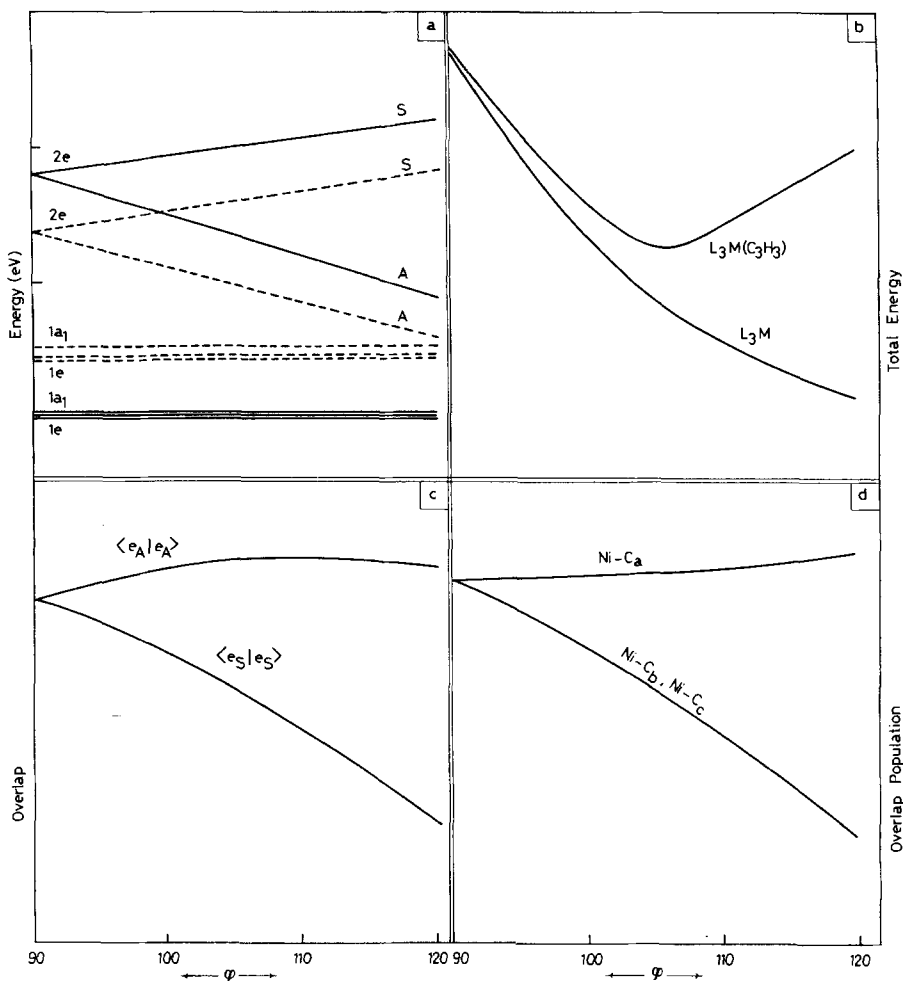


Fig. 5. a) Orbital energy variation in the $Ni(PH_3)_3$ -fragment (solid lines) and in the $[(C_3H_3)Ni(PH_3)_3]^+$ -complex (dashed lines) for the opening of one $P-Ni-P$ angles (φ) from 90° to 120° (The initial C_{3v} -symmetry descends to C_s); b) total energy variation of the $Ni(PH_3)_3$ -fragment and of the $[(C_3H_3)Ni(PH_3)_3]^+$ -complex as a function of the φ angle defined in 4 (The E -value for $Ni(PH_3)$ at $\varphi=90^\circ$ has been arbitrarily made coincident with that of the complex); c) values of the overlap between fragment orbitals as a function of φ ; d) values of the reduced overlap population for Ni, C-bonds as a function of φ .

with respect to the mirror plane of the fragment. To simplify the discussion we have reoriented the coordinate system so that the z -axis lies along one Ni,P-bond. As φ is increased the A-component, shown in 5, is stabilized. The lone pairs move towards the nodal plane of metal- d_{xy} . Important to our later discussion is the fact that there is less hybridization, *i.e.* less mixing of metal- p_y as φ increases to 120° in 5. The (S)-component of the 2e-set behaves differently. First of all it is desta-

bilized as φ increases. At $\varphi = 90^\circ$ it is predominantly metal- d_{z^2} with phosphine lone pairs mixed in an antibonding fashion. There is also some metal- p_z - and p_x -character which is bonding with respect to the phosphine lone pairs. Note that the hybridization of p_x serves to tilt the orbital away from the z -axis (this is illustrated in a somewhat exaggerated fashion in **6**). When φ increases overlap between the lone pairs in the xy -plane and metal- p_x decreases so that at $\varphi = 120^\circ$ the p_x -contribution almost disappears. Thus, the S-component of $2e$ is reoriented to that given by **7** and there is increased mixing of p_z into this orbital.

Figure 5b shows the variation of the total energy of the $\text{Ni}(\text{PH}_3)_3$ -fragment and the cyclopropenium complex as a function of φ . A minimum for the complex is reached at $\varphi = 108^\circ$. With respect to the interaction diagram of *Figure 3*, there is now a smaller energy gap between the S-component of $2e$ and cyclopropenium e'' and a larger one for the A-component. The net result is that the interaction with the S-component is much stronger than that to A. This is only partially counterbalanced by a reduction of the overlap between the S-components of metal- $2e$ and cyclopropenium e'' as φ increases. This is plotted in *Figure 5c* and it is mainly due to the reorientation of the metal orbital (compare **6** with **7**) as well as increasing amounts of p_z . On the other hand, the overlap between the A-components of $2e$ and e'' increases slightly as φ increases. Again this is due to the reduced hybridization of this orbital. As the amount of metal p_y -character decreases the effective angle decreases between the lobes which are directed towards the cyclopropenium ligand and a stronger overlap ensues.

Figure 5d illustrates how the three Ni-cyclopropenium C-overlap populations vary on opening φ . The two Ni, C-bonds, which are *trans* to the two Ni, P-bonds which open, become significantly weaker while the third bond remains constant. This at first sight seems to be contradictory to the results in *Figure 5c*. However, the interaction between the S-components of $2e$ and e'' is dominated by the energy-gap arguments. In the real structure two further geometrical deformations seem to reinforce the Ni, C-bond originally on the mirror plane: the angle between the Ni, P(3) vector and the pseudo- C_3 -axis increases and the Ni(PPh_3)₃-moiety moves towards the C_a -apex of the ring. Both effects serve to increase the overlap between the S-components of the metal- $2e$ and cyclopropenium- e'' . This larger interaction would also suggest that there will be greater charge drift from metal- $2e$ to cyclopropenium- e'' for the S-components. Since this orbital on the cyclopropenium is bonding between C_b and C_c and antibonding to C_a (see *Figure 3c*), the C_b, C_c -bond should be shorter than the other two. Unfortunately the relatively high standard deviations of the C, C-bonds do not allow us to ascertain whether this is indeed true.

The rocking motion of the $\text{Ni}(\text{PH}_3)$ -fragment about the Ni–P(3) as discussed in the previous section was also investigated theoretically. This destroys all symmetry in the complex and a detailed analysis would become unwieldy. Nonetheless, calculations were carried out by keeping φ at 110° and twisting up to 8° about the Ni, P(3)-bond (this is approximately the experimental value). One of the two Ni, C-bonds which have equal overlap populations in C_s -symmetry becomes stronger and the other weaker. In agreement with the results from our crystal structure the stronger bond lies on the same side as the Ni, P-bond which moves

closer to the cyclopropenium ring (in *Figure 2c* this is Ni–C_c and Ni–P(2)). Basically the A-component of metal-2e reorients itself so that one lobe of the d_{xy}-hybrid is directed toward C_c-atom and the other away from C_b-atom. This motion is computed to be energetically very soft and perhaps set in the actual structure by non-bonded contacts.

6. Conclusions and extensions. – The previous analysis shows that closed shell L₃M(C₃H₃)-complexes have a sensible energy gain as the angles L–M–L are opened. In other words the stabilization is inherent to the d¹⁰-L₃M-fragment in its attempt to attain a trigonal conformation. This trend is partially followed even in the presence of polydentate ligands, eventually destroying the C_{3v}-symmetry. Only a ligand with rigid steric requirements such as triphos allows the L₃M-fragment to maintain the true hemioctahedral geometry [2]. In the other cases the overall stabilization of the complex is obtained at expenses of the bond strength between the metal and cyclopropenium. We calculated that the overlap population between the Ni(PH₃)₃- and C₃H₃⁺-fragments drops from 0.486 to 0.128 in the θ -range 90–116° (C_{3v}-symmetry) and from 0.486 to 0.402 when only one L–M–L angle, φ , is allowed to open from 90° to 120° (C_s-symmetry). It is therefore obvious that the triphos ligand is better suited than other sterically less constrained L₃-donors to favor a strong interaction between the metal and a three-membered ring. Actually these concepts may be extended to complexes containing cyclotriphosphorus and cyclotriarsenic units [16]. An analysis of the bonding in complexes of the L₃M(η^3 -P₃)-type is available [17]. Also in this case the strongest bonding interaction is between the metal-2e level and a π^* -orbital of the cycle. We calculated a minimum energy for the model (PH₃)₃Co(η^3 -P₃) at a P_{ligand}–Co–P_{ligand} angle of ca. 100°. Values of 103.6 and 102.7 are found in the complexes (CO)₃Co(η^3 -As₃) [16a] and (np₃)Co(η^3 -P₃) [16d] (np₃ = N(CH₂–CH₂–PPh₂)₃), respectively, while angles of practically 90° are found in all the triphos-containing complexes. This angular value must also control in some way the strength of the metal-to-cycle bonding and the amount of charge drift from the metal to the atoms of the ring which vary their basicity accordingly. The calculations show that the net charge at the P₃-cycle lessens to about 20% of the original value in opening θ from 90° to 100°. We have focused our attention on this point, for the reactivity of the complexes L₃Co(η^3 -P₃) (L₃ = triphos, np₃, 3 CO) is different. In fact in the triphos derivative the P₃-unit is sufficiently basic to react with external metallic electrophilic agents such as Cr(CO)₅- or Mn(CO)₂cp-forming polynuclear derivatives [16e] [18]. Conversely we have repeatedly noticed the low propensity of the np₃-complex toward the same reactions. It has been suggested [19] that the carbonyl derivative (CO)₃Co(η^3 -P₃) also has insufficient electron density on the p-lone-pairs to exhibit the same type of activity.

We thank Mr. *F. Cecconi* for the drawings, Mr. *P. Innocenti* for NMR. measurements and the *Robert A. Welch Foundation* for partial support of this work. *T. Albright* is a *Camille and Henry Dreyfus Teacher-Scholar* (1980–1984) and an *Alfred P. Sloan Research Fellow* (1982–1984). Dr. *T. Albright* thanks the *Istituto di Stereochimica* for a travel grant and generous hospitality.

REFERENCES

- [1] a) C. Mealli, S. Midollini, S. Moneti, L. Sacconi, J. Silvestre & T.A. Albright, *J. Amer. Chem. Soc.* **104**, 95 (1982); b) C. Mealli, S. Midollini, S. Moneti & L. Sacconi, *Angew. Chem. Int. Ed.* **19**, 931 (1980).
- [2] C. Mealli, S. Midollini, S. Moneti & L. Sacconi, *J. Organomet. Chem.* **205**, 273 (1981).
- [3] L. Sacconi & R. Morassi, *J. Chem. Soc. A* **1968**, 2997.
- [4] 'Philips Serving Science and Industry', N. 20, 1972, p. 18.
- [5] a) R.J. Hoffmann, *J. Chem. Phys.* **39**, 1397 (1963); b) R.J. Hoffmann & W.N. Lipscombe, *ibid.* **36**, 3179, 3489 (1962); **37**, 2872 (1962); c) J.H. Ammeter, H.B. Bürgi, J.C. Thibeault & R. Hoffmann, *J. Amer. Chem. Soc.* **100**, 3686 (1978).
- [6] T.J. Mazanec, D.T. Kwolianski & D.W. Meek, *Inorg. Chem.* **19**, 85 (1980).
- [7] M. Di Vaira, S. Midollini & L. Sacconi, *Inorg. Chem.* **18**, 3466 (1979).
- [8] E.D. Jemmis & R. Hoffmann, *J. Amer. Chem. Soc.* **102**, 2750 (1980).
- [9] R. Hoffmann, J.R. Swenson & C.C. Wan, *J. Amer. Chem. Soc.* **95**, 7644 (1973); H. Fujimoto & R. Hoffmann, *J. Phys. Chem.* **78**, 1167 (1974).
- [10] a) M. Elia & R. Hoffmann, *Inorg. Chem.* **14**, 1058 (1975); b) A. Dedieu, T.A. Albright & R. Hoffmann, *J. Amer. Chem. Soc.* **101**, 3141 (1979).
- [11] T. Chiang, R.C. Kerber, S.D. Kimball & J.W. Lauher, *Inorg. Chem.* **18**, 1687 (1979).
- [12] M. Elia, M.M. Chen, D.M.P. Mingos & R. Hoffmann, *Inorg. Chem.* **15**, 1149 (1976).
- [13] T.A. Albright, R. Hoffmann & P. Hofmann, *J. Amer. Chem. Soc.* **99**, 7546 (1977).
- [14] R. Hoffmann, *Acc. Chem. Res.* **4**, 1 (1971).
- [15] R.M. Tuggle & D.L. Weaver, *Inorg. Chem.* **10**, 1504 (1971).
- [16] a) A.L. Foust, M.S. Foster & L.F. Dahl, *J. Amer. Chem. Soc.* **91**, 5631 (1969); b) A. Vizi-Orosz, *J. Organomet. Chem.* **111**, 61 (1976); c) C.A. Ghilardi, S. Midollini, A. Orlandini & L. Sacconi, *Inorg. Chem.* **19**, 301 (1980); d) F. Cecconi, P. Dapporto, S. Midollini & L. Sacconi, *Inorg. Chem.* **17**, 3292 (1978); e) C.A. Ghilardi, S. Midollini, A. Orlandini & L. Sacconi, *Inorg. Chem.* **19**, 301 (1980); f) C. Bianchini, C. Mealli, A. Meli & L. Sacconi, *Inorg. Chim. Acta* **37**, L543 (1979); g) P. Dapporto, P. Stoppioni, L. Sacconi & F. Zanobini, *Inorg. Chem.* **20**, 3834 (1981).
- [17] M. Di Vaira & L. Sacconi, *Angew. Chem. Int. Ed.* **21**, 330 (1982).
- [18] C. Mealli, S. Midollini, S. Moneti & L. Sacconi, *Cryst. Struct. Commun.* **9**, 1017 (1980).
- [19] A. Vizi-Orosz, V. Galamb, G. Palyi & L. Markó, *J. Organomet. Chem.* **216**, 105 (1981).